[^{99m}Tc]Demotate 2 in the detection of sst_2-positive tumours: a preclinical comparison with [^{111}In]DOTA-tate

Theodosia Maina[1], Berthold A. Nock[1], Paul Cordopatis[2], Bert F. Bernard[3], Wout A. P. Breeman[3], Arthur van Gameren[3], Ria van den Berg[3], Jean-Claude Reubi[4], Eric P. Krenning[3], Marion de Jong[3]

[1] Institute of Radioisotopes - Radiodiagnostic Products, National Center for Scientific Research "Demokritos", 153 10 Ag. Paraskevi Attikis, Athens, Greece
[2] Department of Pharmacy, University of Patras, Patras, Greece
[3] Department of Nuclear Medicine, Erasmus MC, Rotterdam, The Netherlands
[4] Division of Cell Biology and Experimental Cancer Research, Institute of Pathology, University of Berne, Berne, Switzerland

Received: 8 February 2005 / Accepted: 12 December 2005 / Published online: 28 March 2006

Abstract. *Purpose:* The aim of this study was to evaluate [^{99m}Tc]Demotate 2 ([^{99m}Tc-N_4^{0-1},Asp^0,Tyr^3]octreotate) as a candidate for in vivo imaging of sst_2-positive tumours and to compare it with [^{111}In]DOTA-tate ([^{111}In-DOTA^0, Tyr^3]octreotate).
Methods: Labelling of Demotate 2 with ^{99m}Tc was performed at room temperature using $SnCl_2$ as reductant in the presence of citrate at alkaline pH. Radiochemical analysis involved ITLC and HPLC methods. Peptide conjugate affinities for sst_2 were determined by receptor autoradiography on rat brain cortex sections using [DOTA^0,^{125}I-Tyr^3]octreotate as the radioligand. The affinity profile of Demotate 2 for human sst_1–sst_5 was studied by receptor autoradiography in cell preparations using the universal somatostatin radioligand [^{125}I][Leu^8,(D)Trp^{22}, Tyr^{25}]somatostatin-28. The internalisation rates of [^{99m}Tc]Demotate 2 and [^{111}In]DOTA-tate were compared in sst_2-positive and -negative control cell lines. Biodistribution of radiopeptides was studied in male Lewis rats bearing CA20948 tumours.
Results: Peptide conjugates showed selectivity and a high affinity binding for sst_2 (Demotate 2 IC_{50}=3.2 n*M* and DOTA-tate IC_{50}=5.4 n*M*). [^{99m}Tc]Demotate 2, like [^{111}In] DOTA-tate, internalised rapidly in all sst_2-positive cells tested, but not in sst_2-negative control cells. After injection in CA20948 tumour-bearing rats both radiopeptides showed high and specific uptake in the sst_2-positive organs and in the implanted tumour and rapid excretion from non-target tissues via the kidneys.
Conclusion: [^{99m}Tc]Demotate 2, similarly to the known sst_2-targeting agent [^{111}In]DOTA-tate, showed promising biological qualities for application in the scintigraphy of sst_2-positive tumours.

Keywords: Tetraamine – DOTA – sst_2 targeting – radiolabelled [Tyr^3]octreotate

Eur J Nucl Med Mol Imaging (2006) 33:831–840
DOI 10.1007/s00259-006-0068-8

Theodosia Maina (✉)
Institute of Radioisotopes - Radiodiagnostic Products,
National Center for Scientific Research "Demokritos",
153 10 Ag. Paraskevi Attikis,
Athens, Greece
e-mail: mainathe@rrp.demokritos.gr
Tel.: +30-210-6503908, Fax: +30-210-6524480

Introduction

Somatostatin receptor (sst) scintigraphy with [^{111}In-DTPA^0] octreotide (OctreoScan) has become a powerful tool in the diagnosis and staging of neuroendocrine tumours which express somatostatin subtype 2 receptors (sst_2) [1–3]. Furthermore, significant advances have been made in sst_2-targeted radionuclide tumour therapy using somatostatin analogues functionalised with the universal chelator DOTA (DOTA=1,4,7,10-tetraazacyclododecane-1,4,7,10-tetraacetic acid) and labelled with therapeutic radionuclides, like ^{111}In, ^{90}Y or the radiolanthanides [2–6]. The therapeutic efficacy of such ^{111}In, ^{90}Y or ^{177}Lu labelled somatostatin analogues can be predicted by the percentage of radioactivity accumulation in tumour deposits, illustrating the fact that somatostatin receptor status imaging in primary and metastatic lesions in the patient has a significant impact in therapy planning and follow-up [7]. As a cyclotron-produced radionuclide, ^{111}In is available at a relatively high cost and requires more sophisticated distribution and hospital logistics for routine application. In addition, the sub-optimal nuclear properties of ^{111}In (medium-energy photons, Auger electron emission) lead to inferior image quality and to higher radiation doses to patients [2].

To circumvent these drawbacks, several investigators have been searching for somatostatin analogues based on ^{99m}Tc instead [8, 9]. The cost-effectiveness and wide availability of ^{99m}Tc, which is readily accessible in high purity by elution of commercial generators, along with its ideal nuclear properties ($t_{1/2}$=6 h, gamma photons of 140 keV), which lead to high-quality imaging and minimal radiation burden to patients, have made ^{99m}Tc the most widely used radionuclide in diagnostic nuclear medicine. It should be added that the prospect of implementing a 1-day clinical protocol by means of a ^{99m}Tc-based somatostatin radiotracer that rapidly localises at tumour sites is most attractive and will certainly increase the practical convenience of using ^{99m}Tc. Furthermore, owing to the similarities of technetium and rhenium chemistries, the use of diagnostic ^{99m}Tc/therapeutic ^{188}Re somatostatin-based radiopeptide pairs in the scintigraphic detection and treatment of sst_2-positive tumours is a highly desirable but still open option [8, 9]. Aiming toward this goal, several ^{99m}Tc-labelled somatostatin analogues have been developed so far. Most of these molecules are based on octreotide or other cyclic somatostatin peptide analogues and are modified at the N-terminus with a large variety of chelators to ensure stable binding of ^{99m}Tc [8]. Thus, tetradentate triamedethiol (N_3S) [10, 11] or mixed-ligand HYNIC/EDDA-tricine [12–14] systems (HYNIC=hydrazinonicotinamide, EDDA=ethylenediamine-*N*,*N*′-diacetic acid, tricine=*N*-[tris(hydroxymethyl)]glycine) stabilising the metal at oxidation state +5 have led to promising radiotracers that are either already commercially available or are currently undergoing clinical evaluation [8–14].

We have recently reported on [^{99m}Tc]Demotate 1, a [Tyr^3]octreotate analogue functionalised at the N-terminus with an open chain tetraamine for stable ^{99m}Tc binding [15–17]. This donor atom set was selected owing to previous reports on its ability to form stable monocationic polar complexes with technetium and rhenium [18–21] while the corresponding ^{99m}Tc-chelate is easily produced in specific activities suitable for receptor targeting applications [20]. These qualities could be confirmed in [^{99m}Tc]Demotate 1. The agent showed high affinity for sst_2 in vitro and a high tumour uptake in pathological animal models [15] and in patients [16, 17]. The positive charge of the metal chelate at the N-terminus of the peptide is suspected to have favoured receptor binding and tumour uptake of [^{99m}Tc]Demotate 1.

In this work we report on [^{99m}Tc-N_4^{0-1},Asp^0,Tyr^3] octreotate, [^{99m}Tc]Demotate 2, wherein an Asp residue—containing a pendant negatively charged carboxylate group—has been introduced between the monocationic metal chelate and the N-terminal amino acid of the original [^{99m}Tc]Demotate 1 sequence. The in vitro properties of [^{99m}Tc]Demotate 2 (binding affinity for sst_2, internalisation/externalisation behaviour) were studied in several sst_2-positive and -negative control cell lines. Results were evaluated in comparison with [^{111}In-DOTA^0,Tyr^3]octreotate ([^{111}In]DOTA-tate), a thoroughly investigated [Tyr^3] octreotate derivative exhibiting superior biological properties compared with the commercial agent OctreoScan [14, 22–24]. The biodistribution of the two radiotracers in male Lewis rats carrying the CA20948 tumour model and their renal accumulation pattern are compared and discussed. Eventually, conclusions about the suitability of [^{99m}Tc] Demotate 2 as a radiotracer in the targeted imaging of sst_2-positive tumours are drawn.

Materials and methods

Synthesis of peptides

Synthesis of Demotate 2 was performed on the solid support [15]. In brief, the nonapeptide sequence Asp-(D)Phe-Tyr-(D)Trp-Lys-Thr-Cys-Thr-OH was assembled on the acid-sensitive 2-chlorotrityl chloride resin (0.6 mmol/g substitution) following Fmoc protection methodology and using the amino acid precursors Fmoc-Asp(^{t}Bu), Fmoc-(D)Phe, Fmoc-Cys(Mmt), Fmoc-Tyr(^{t}Bu), Fmoc-Thr(^{t}Bu), Fmoc-Lys(Boc) and Fmoc-(D)Trp(Boc). Amino acid coupling was achieved by reaction with a 3 molar excess of N^{α}-fluorenylmethyloxycarbonyl-amino acid, a 4.5 molar excess of 1-hydroxybenzotriazol and a 3.3 molar excess of diisopropylcarbodiimide in dimethylformamide (DMF) for 3 h. Completeness of coupling reactions was monitored by the Kaiser test and the Fmoc groups were removed by treatment with 20% piperidine in DMF for 30 min. *N*,*N*′,*N*″,*N*‴-tetra-(*tert*-butoxycarbonyl)-6-(carboxy)-1,4,8,11 -tetraazaundecane was eventually coupled at the N-terminus Asp of the resin-immobilised sequence by reacting in a 3 molar excess in the presence of a 3.3 molar excess of HATU (*o*-(7-azabenzotriazolyl-1,1,3,3-tetramethyluronium hexafluorophosphate)) and a 7 molar excess of diisopropylamine in DMF for 2 h. The peptide conjugate was detached from the solid support free of lateral protecting groups after 5 h treatment in a trifluoroacetic acid (TFA)/DCM/1,2-ethanedithiol/H_2O/anisole solution (8/1/0.7/0.2/0.1, 20 ml/g peptide resin) at room temperature. This mixture was concentrated to a small volume and the conjugate was precipitated with ether. Cyclisation was achieved by a 72-h incubation in 20% aqueous DMSO (3 ml/mg conjugate). The crude product was initially purified over a Sephadex G-15 column eluted with 0.2 *M* acetic acid and finally by semi-preparative high-performance liquid chromatography (HPLC) on an RP C-18 cartridge (Phase Sep C-18 S10 ODS2) run with a linear gradient A/B 90%/10% to 20%/80% (A=0.1% TFA in water, B=0.1% TFA in acetonitrile) within 30 min at a flow rate of 2 ml/min.

Overall yield: 35%; t_R HPLC sys1: 17.2 min (sys1=Techsphere 5 ODS2 C-18 HPLC Technology column, 4.6 mm × 250 mm, run at a 2 ml/min flow rate with a linear gradient system A/B 90%/10% to 20%/80% over 30 min, A=0.1% TFA in water, B=0.1% TFA in acetonitrile); t_R HPLC sys2: 16.5 min (sys2=RP-18 Symmetry Shield Waters column, 5 μm, 3.9 mm × 150 mm, run at a 1 ml/min flow rate with a linear gradient system starting from 90% A/10% B and advancing to 60% A/40% B within 30 min, with solvent A=0.1% trifluoroacetic acid in water and B=pure acetonitrile); ES-MS: 1350.8 ([M^+], 87), 676.0 ([MH^{2+}], 100).

DOTA-tate [22, 24] was provided by BioSynthema (St. Louis, MO, USA). t_R HPLC sys2: 18.3 min.

Peptide radiolabelling

For ^{99m}Tc labelling [15], $^{99m}TcO_4^-$ eluate (420 μl, 370-740 MBq) from a ^{99}Mo/^{99m}Tc generator (Tyco Healthcare, Petten, The Netherlands) was transferred in an Eppendorf vial. Fifty microlitres of a 0.5 *M* Na_2HPO_4 pH 11.5–12 buffer was added, followed by 0.1 *M* citrate solution (5 μl), 10^{-3} *M* Demotate 2 stock solution (15 μl,

15 nmol) and a freshly prepared solution of $SnCl_2 \cdot 2H_2O$ in ethanol (15 µl, 30 µg, 157 nmol). After 30-min incubation at room temperature, the mixture pH was adjusted to 7.4 by addition of 1 *M* HCl.

For ^{111}In labelling [24], $^{111}InCl_3$ (Tyco Healthcare, Petten, The Netherlands) was provided in 0.01–0.2 *N* HCl and 370–740 MBq was used. Labelling was conducted by adding a 10^{-3} *M* stock solution of [DOTA^0,Tyr^3]octreotate in 10–50 m*M* acetate buffer and 2.5 m*M* sodium ascorbate in 5 m*M* sodium acetate in a total volume of 40–75 µl in a double-sealed vial (Mobitec, ITK Diagnostics, Uithoorn, The Netherlands). Typical end pH was in the range 4–4.5. Labelling was completed after heating at 100°C in a temperature-controlled heating block for 25 min. The preparation of [DOTA^0,^{125}I-Tyr^3]octreotate used in competition binding assays followed the method previously described for [DOTA^0,^{125}I-Tyr^3]octreotide [25].

Quality control

Formation and radiochemical purity of [^{99m}Tc]Demotate 2 was monitored both by instant thin-layer chromatography (ITLC) and by HPLC, as described previously [15]. Briefly, HPLC analyses were conducted on an RP Symmetry Shield column (5 µm, 3.9 mm × 150 mm) from Waters, applying a linear gradient system at a 1 ml/min flow rate starting from 10% B and advancing to 40% B within 30 min, with solvent A=0.1% TFA in water and B=pure acetonitrile. For ITLC, samples (<1 µl) were applied on ITLC-SG strips, developed up to 10 cm from the origin with 1 *M* ammonium acetate/MeOH 1/1 (v/v). Strips were left to dry in the open and then were scanned on an ITLC scanner, model VCS-101 from Veenstra (Joure, The Netherlands), and/or cut into two pieces: 1st=Start (origin + 0.5–1 cm): $^{99m}TcO_2$ and 2nd=Front (the rest of the strip): $^{99m}TcO_4^-$ [^{99m}Tc]citrate and [^{99m}Tc]Demotate 2. Pieces were measured for their radioactivity content in the gamma counter, as previously described [15]. Quality control of the [^{111}In-DOTA^0,Tyr^3]octreotate labelled product was performed by HPLC and ITLC as well. HPLC analyses were performed under the same conditions as for [^{99m}Tc]Demotate 2. For ITLC tests, samples were mixed with a threefold volume amount of 4 m*M* DTPA pH 4, placed on an ITLC-SG strip and eluted with 0.1 *M* Na-citrate pH 5. Strips were scanned on the ITLC scanner. Under these conditions, R_f [^{111}In-DOTA^0,Tyr^3]octreotate: 0–0.1, while R_f free ^{111}In: 0.9–1.0. Samples from both radiopeptide labelling mixtures were analysed up to 24 h post labelling.

Receptor affinity

The affinities of Demotate 2 and DOTA-tate for sst_2 were tested by receptor autoradiography on 10 µm frozen rat brain cortex sections using [DOTA^0,^{125}I-Tyr^3]octreotate as the radioligand, as previously described [22, 25]. As affinities of the previously reported Demotate 1 (and [^{99m}Tc/^{99g}Tc]Demotate 1) for sst_2 were extracted from experiments with AR4-2J membranes using a different radioligand ([^{125}I-Tyr^3]octreotide) [15], Demotate 1 was also included in this study for the purpose of comparison. The radioligand was incubated with increasing concentrations (ranging from 10^{-12} to 10^{-6} *M*) of each conjugate in binding buffer (167 m*M* Tris, pH 7.6, 5 m*M* $MgCl_2$, 40 µg/ml bacitracin, 1% BSA) on consecutive brain sections at room temperature for 1 h. Slides were rinsed for 5 min with chilled buffer A (167 m*M* Tris, pH 7.6, 5 m*M* $MgCl_2$, 40 µg/ml bacitracin, 0.25% BSA) and B (167 m*M* Tris, pH 7.6, 5 m*M* $MgCl_2$, 40 µg/ml bacitracin). They were dried and exposed to phosphor imaging screens (Packard Instruments Co., Meriden, CT, USA) over 24 h in X-ray cassettes and analysed using a Cyclone phosphor imager and a computer-assisted Opti-Quant 03.00 image processing system (Packard Instruments Co., Groningen, The Netherlands). The respective IC_{50} values were calculated using the Graph Pad Software (San Diego, CA, USA). Experiments were performed in triplicate.

Determination of sst_{1-5} affinity profile of Demotate 2

Cells stably expressing human sst_{1-5} were grown, as previously reported [4]. Cell membrane pellets were prepared and receptor autoradiography was performed on pellet sections (mounted on microscope slides), as previously detailed [4]. Complete displacement experiments were conducted using the universal somatostatin radioligand [^{125}I][Leu^8,(D)Trp^{22},Tyr^{25}]somatostatin-28 and increasing concentrations of Demotate 2 or the reference peptide somatostatin-28 (SS-28) ranging from 0.1 to 1,000 n*M*. Tissue standards (autoradiographic [^{125}I]microscales, Amersham, UK) containing known amounts of radionuclides, cross-calibrated to tissue-equivalent ligand concentrations, were used for quantification [4] and IC_{50} values were calculated using a computer-assisted image processing system.

Cell culture

Sst_2-positive CA20948 cells [26] were cultured from the solid CA20948 rat pancreatic tumour and were grown in DMEM (Gibco, Life Technologies) supplemented with 10% heat-inactivated fetal bovine serum, 2 m*M* glutamine, 1 m*M* sodium pyruvate, fungizone (0.1 mg/l) and 50 IU/ml penicillin/streptomycin. Sst_2-positive rat pancreatic AR4-2J cells [27, 28] (CAMR, Wiltshire, UK) were grown in RPMI-1640 (Gibco, Life Technologies) supplemented with 10% heat-inactivated fetal bovine serum, 2 m*M* glutamine, 1 m*M* sodium pyruvate, fungizone (0.1 mg/l) and 50 IU/ml penicillin/streptomycin. Sst_2-transfected Mat B cells and sst_2-transfected CHO cells (provided by Dr. J. E. Bugaj, Tyco, St. Louis, MO, USA) were grown in RPMI (Gibco, Life Technologies) supplemented with 10% heat-inactivated fetal bovine serum, 2 m*M* glutamine, 1 m*M* sodium pyruvate, fungizone (0.1 mg/l), 50 IU/ml penicillin/streptomycin and 10,000 U/l gentamycin. Subconfluent cell cultures were transferred to six-well plates 24 h before the cell uptake and internalisation experiments.

Internalisation

For internalisation experiments the sst_2-positive cell lines CA20948, AR4-2J, CHO(sst_2+) and Mat B(sst_2+) were employed along with the ARO sst_2-negative controls [26–28]. Cells grown in six-well plates were washed with 2×1 ml PBS (37°C). Cells were incubated at 37°C with either [^{99m}Tc]Demotate 2 or [^{111}In]DOTA-tate in 1 ml incubation medium (RPMI supplemented with 1% BSA and 20 m*M* Hepes, pH 7.4) containing 10^{-10} *M* total peptide conjugate and 40 kBq of each radiolabelled peptide over time or for 1 h in the presence of increasing concentrations of octreotide. In parallel, cells were also incubated with excess octreotide (10^{-6} M) to determine non-specific internalisation. Internalisation was interrupted by removing the medium and washing twice with 2 ml PBS (4°C). Surface-bound radioactivity was removed by a 10-min treatment of intact cells with 1 ml 20 m*M* sodium acetate (pH 5.0) at room temperature. Internalised activity was collected after lysing the cells with 1 ml 0.1 *M* NaOH. The radioactivity content of collected fractions was measured in a LKB-1282 Compugamma system counter and expressed as a percentage of the applied dose per mg cell protein.

The latter was determined using a commercial kit (BioRad, The Netherlands). Experiments were performed four times in triplicates.

Externalisation experiments

The externalisation properties of [^{99m}Tc]Demotate 2 and [^{111}In]DOTA-tate from CA20948 cells were studied by incubating cells with each radiopeptide for 60 min at 37°C. Incubation was terminated by washing the cells twice with 2 ml ice-cold PBS. Incubation of the cells in PBS–20 m*M* sodium acetate (pH 5.0) at ambient temperature for 10 min was performed to remove unbound and membrane-bound ligand. After washing again with PBS, externalisation started by addition of 1 ml medium (RPMI 1640 with Glutamax supplemented with 20 m*M* Hepes, 10 m*M* Pipes, 1% heat-inactivated fetal bovine serum pH 7.4) and incubation at 37°C for 10, 60, 120 and 180 min. Incubation was stopped by medium collection (medium fraction). The cells were washed with PBS and the surface-bound fraction was collected after reaction for 10 min with 1 ml PBS–20 m*M* sodium acetate (pH 5.0). The cells were lysed with 1 ml 0.1 *M* NaOH and collected (cell fraction). The radioactivity contents of medium, surface-bound fraction and cell fraction were measured in a LKB-1282 Compugamma system counter and expressed as a percentage of the applied dose per milligram cell protein. After counting the radioactivity, protein was measured in lysed cells using a commercial kit (BioRad, The Netherlands). Externalisation experiments were performed twice in triplicate.

Tissue distribution

All animal studies were conducted in compliance with the Animal Welfare Committee requirements of the Erasmus MC and with generally accepted guidelines governing such work. The rat pancre-

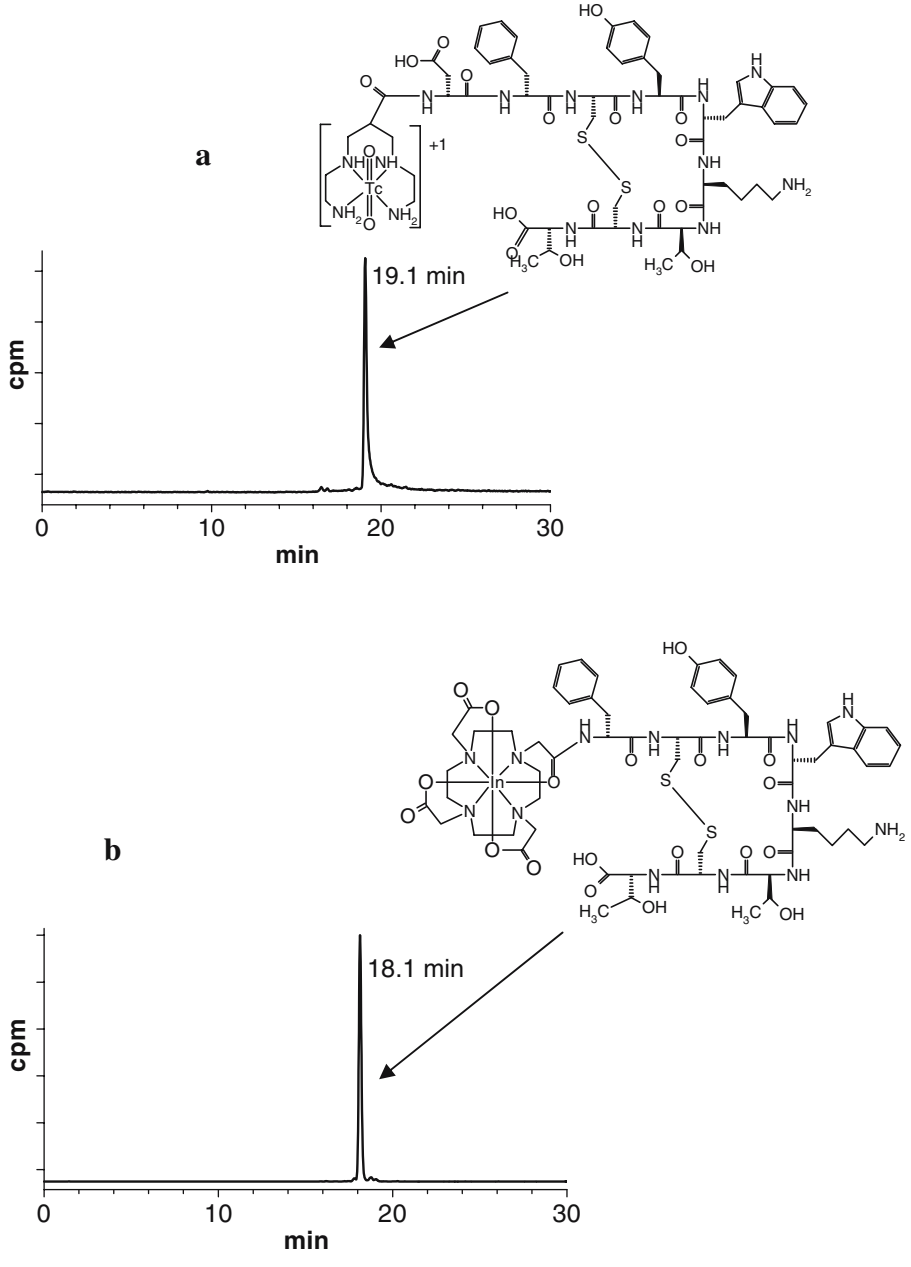

Fig. 1. Typical HPLC analysis of [^{99m}Tc]Demotate 2 (**a**) and [^{111}In]DOTA-tate (**b**) labelling mixtures. Runs were performed on an RP Symmetry Shield Waters column (5 μm, 3.9 mm×150 mm) at a 1 ml/min flow rate with a linear gradient system starting from 90% A/10% B and advancing to 60% A/40% B within 30 min (A=0.1% trifluoroacetic acid in water and B=pure acetonitrile)

atic CA20948 tumour was grown in the flank of male Lewis rats (Harlan, The Netherlands; 80–120 g) [26]. Palpable tumours were grown 2–3 weeks after inoculation of a CA20948 cell suspension (2–5×10^6 cells). A bolus (500 µl) containing [^{99m}Tc]Demotate 2 (6 MBq/0.5 µg peptide) and [^{111}In]DOTA-tate (3 MBq/0.5 µg peptide) was administered via the dorsal vein of the penis [22]. In a separate series of rats, 500 µg of octreotide was injected along with the radiopeptides in order to determine the non-specific accumulation at the target site (blocked animals). Animals were sacrificed in groups of four at 1, 4 or 24 h post injection (p.i.). Blood and tissue samples were collected and weighed. Their radioactivity content corresponding to ^{99m}Tc and to ^{111}In was measured in a gamma counter (Perkin-Elmer, Groningen, The Netherlands) in two separate energy windows (125–155 keV for ^{99m}Tc and 160–190 keV and 220–275 keV for ^{111}In). Statistical analysis was performed using the Student's *t* test (Graph Pad Software, San Diego, CA, USA) and a *p* value <0.05 was considered statistically significant.

Kidney autoradiography

The distribution of radioactivity in the kidneys of male Lewis rats injected with [^{99m}Tc]Demotate 2 (6 MBq/0.5 µg peptide) and [^{111}In]DOTA-tate (3 MBq/0.5 µg peptide) was tested employing ex vivo autoradiography [22]. Briefly, kidneys were excised 4 h after injection of [^{99m}Tc]Demotate 2 and at 24 h after injection of [^{111}In]DOTA-tate, embedded in TissueTek and prepared for cryosection. Kidney sections of ~10 µm each were mounted on glass plates. Sections were exposed to phosphor imaging screens (Packard Instruments Co., Meriden, CT, USA) over 24 h in X-ray cassettes and analysed using a Cyclone phosphor imager and a computer-assisted Opti-Quant 03.00 image processing system (Packard Instruments Co., Groningen, The Netherlands).

Results

Radiotracers

Incorporation of ^{99m}Tc by Demotate 2 and ^{111}In by DOTA-tate was ≥99%, as confirmed by ITLC and HPLC methods. A typical HPLC radiochromatogram for the [^{99m}Tc]Demotate 2 labelled product is presented in Fig. 1a showing the bulk of radioactivity eluting as a single peak (t_R=19.1 min) with no trace amounts of $^{99m}TcO_4^-$ (t_R=3.5 min) or [^{99m}Tc]citrate (t_R=1.8–2.3 min). At the same time, recovery of radioactivity from the column was ≥96%. This finding, in combination with results from ITLC tests revealing typical radioactivity percentages <1% at the origin, ruled out the formation of $^{99m}TcO_2$. Data obtained from ITLC analysis of the [^{111}In]DOTA-tate tracer revealed a similarly high purity of the forming radiopeptide (Fig. 1b). Typical specific activities of 37 MBq/nmol attained for [^{99m}Tc]Demotate 2 and 370 MBq/nmol for [^{111}In]DOTA-tate were well within the range required for sst_2-targeted applications [2, 8, 12].

Receptor binding studies

The radioligand [DOTA^0,^{125}I-Tyr^3]octreotate was displaced from somatostatin binding sites in rat brain cortex sections in a monophasic and dose-dependent manner by Demotate 1, Demotate 2 or DOTA-tate. The IC_{50} values calculated using the same methodology for these three compounds were 1.8 n*M*, 3.2 n*M* and 5.4 n*M*, respectively. Representative displacement curves for Demotate 2 and DOTA-tate are shown in Fig. 2.

sst_{1-5} affinity profiles

The IC_{50} values of Demotate 2 for the five somatostatin receptor subtypes are included in Table 1, while the corresponding values for DOTA-tate and its metallated analogues have been reported elsewhere [4]. Results were extracted from complete displacement experiments with the universal somatostatin radioligand [^{125}I][Leu^8,(D)Trp^{22}, Tyr^{25}]somatostatin-28 on membranes from cells expressing the receptor subtypes. Demotate 2 bound specifically to sst_2 with an IC_{50} value of 3.2 n*M*, showing only very low affinity for the sst_4 (IC_{50}>300 n*M*) and the sst_5 (IC_{50}>145 n*M*) and no affinity for the sst_1 and sst_3 (IC_{50}>1,000 n*M*).

Internalisation experiments

The internalisation of [^{99m}Tc]Demotate 2 and [^{111}In]DOTA-tate in sst_2-positive cells [CA90248, AR4-2J, Mat B (sst_2+) and CHO (sst_2+)] was rapid and receptor-specific for both compounds, as shown in Fig. 3. In contrast, in sst_2-negative control cells the radioactivity was not internalised.

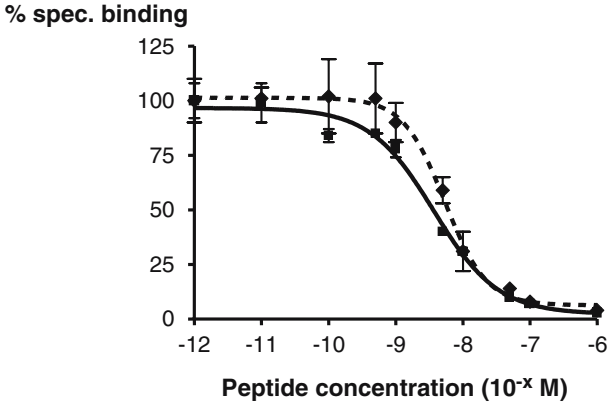

Fig. 2. Comparative displacement curves of [DOTA^0,^{125}I-Tyr^3]octreotate from somatostatin binding sites in rat brain cortex sections by increasing concentrations of Demotate 2 (■, *solid line*) and DOTA-tate (◆, *dashed line*)

Table 1. Affinity profiles (IC_{50}) of Demotate 2 and somatostatin-28 (SS-28, control) for human (h) sst_{1-5} receptors

Analogue	$hsst_1$	$hsst_2$	$hsst_3$	$hsst_4$	$hsst_5$
SS-28	2.2; 1.3	3.2; 3.2	4; 4.8	5.2; 4.3	2.6; 1.5
Demotate 2	>1,000; 772	3.1; 3.4	>1,000 (2)	312; 340	158; 145

IC_{50} values are in n*M* and number of independent studies are given in parentheses

Externalisation experiments

The rate of externalisation for [^{99m}Tc]Demotate 2 and [^{111}In]DOTA-tate from CA20948 cells is compared in Fig. 4. The radiopeptides were allowed to internalise for 1 h at 37°C, at which point internalisation was taken as maximum (100%). A slow efflux of radioactivity from cells over time resulted in a circa 60% residual activity at 3-h incubation for both radiopeptides.

Animal studies

Comparative data of [^{99m}Tc]Demotate 2 and [^{111}In]DOTA-tate biodistribution in male CA20948 tumour-bearing Lewis rats are summarised in Tables 2 and 3, respectively. Blood clearance was very rapid for both radiotracers, with blood values as low as 0.13%ID/g as early as 1 h p.i. The radioactivity was rapidly cleared from muscle and non-target tissues, mainly via the kidneys and the urinary system. Although no striking differences in biodistribution were observed between [^{99m}Tc]Demotate 2 and [^{111}In]DOTA-tate, overall [^{111}In]DOTA-tate cleared more efficiently from background tissues. Thus, [^{99m}Tc]Demotate 2 showed higher values in liver, spleen and kidney at 1 h p.i. The kidney uptake, in particular, was found to be ~20% higher at 1 h p.i. and 68% higher at 4 h p.i. than the corresponding [^{111}In]DOTA-tate uptake. However, during the following 20 h, kidney radioactivity washed out more efficiently in the case of [^{99m}Tc]Demotate 2.

In the somatostatin receptor-rich organs, such as the pancreas, the adrenals, the pituitary and the gastrointestinal tract, both [^{99m}Tc]Demotate 2 and [^{111}In]DOTA-tate exhibited high uptake. Again, [^{99m}Tc]Demotate 2 displayed significantly higher values during the initial time intervals (1 h and 4 h p.i.), with [^{111}In]DOTA-tate showing slower washout from these tissues over 24 h. Localisation of both radiotracers in the sst_2-positive tissues could be reduced by >90% in the animals receiving a high dose of unlabelled peptide (500 μg octreotide) and was therefore considered to be receptor mediated. For example, the pancreas uptake of 8.60±1.25%ID/g for [^{99m}Tc]Demotate 2 at 4 h p.i. reached only 0.37±0.08%ID/g in the group of blocked animals.

Accumulation of [^{99m}Tc]Demotate 2 and [^{111}In]DOTA-tate in the CA20948 tumour did not show significant differences during the initial time points. However, 24 h after administration, tumour values for [^{111}In]DOTA-tate were found to be 62% higher than those for the ^{99m}Tc-peptide. Tumour uptake for both radiotracers was shown to be a receptor-mediated process by means of the >90% reduction observed in the tumour uptake of blocked animals.

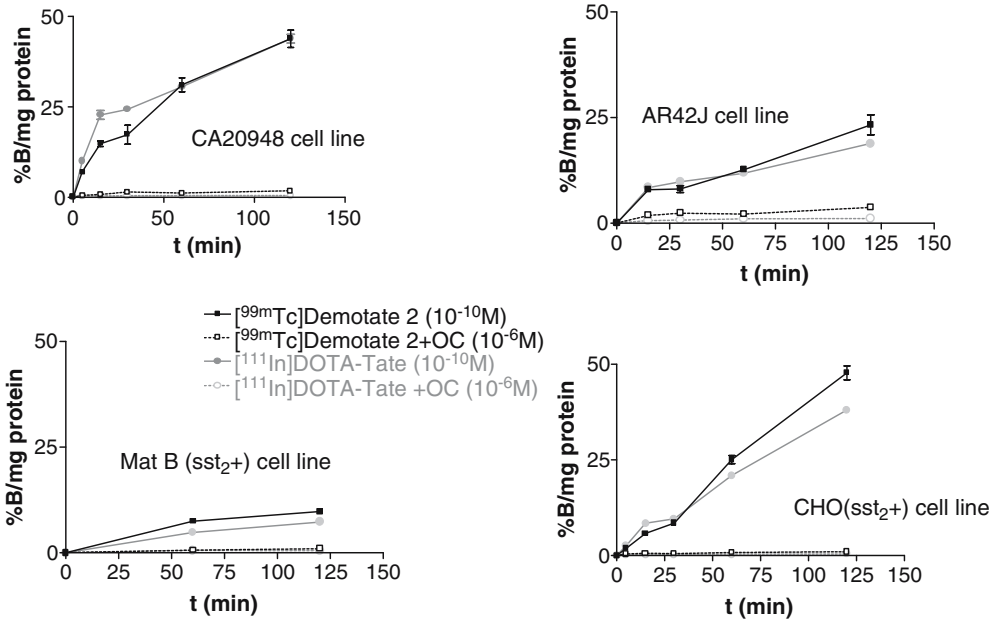

Fig. 3. Comparative time-dependent internalisation of [^{99m}Tc]Demotate 2 (total peptide conjugate 10^{-10} *M*) and [^{111}In]DOTA-tate (total peptide conjugate 10^{-10} *M*) at 37°C in the sst_2-expressing cell lines CA20948, AR4-2J, Mat B (sst_2+) and CHO (sst_2+) in the absence (*solid symbols*, specific) or presence (*open symbols*, non-specific) of competing octreotide (*OC*, 10^{-6} *M*)

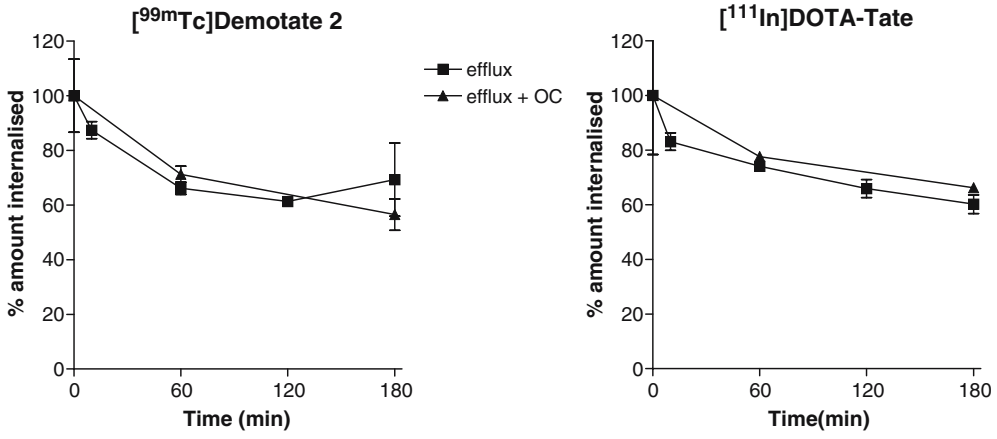

Fig. 4. Comparison of efflux rates of [^{99m}Tc]Demotate 2 and [^{111}In]DOTA-tate from CA20948 cells at 37°C without or with addition of 10^{-6} M octreotide (*OC*) to prevent re-internalisation

Ex vivo kidney autoradiography

Representative ex vivo autoradiographs of rat kidneys 4 h after injection of [^{99m}Tc]Demotate 2 and 24 h after injection of [^{111}In]DOTA-tate are compared in Fig. 5. Although the rat kidney does not express sst_2, a high amount of renal radioactivity was detected, especially in the case of [^{99m}Tc]Demotate 2. This is most probably attributable to the reabsorption of radiopeptides in the cells of the proximal tubules after glomerular filtration [29, 30]. Most of the kidney radioactivity was localised in the renal cortex, with a much lower portion detected in the outer medulla. Thus, radioactivity in the outer medulla was found to be about 60% of cortical radioactivity whereas in the inner medulla and pelvis, no radioactivity was found. This distribution pattern was very similar for the two radiopeptides tested at 4 h and 24 h p.i. It is interesting to note that at 24 h p.i. the pattern of radioactivity distribution remained unchanged for [^{111}In]DOTA-tate, concordant with the prolonged renal uptake observed for this agent during biodistribution.

Discussion

We have previously reported on [^{99m}Tc]Demotate 1, a [Tyr^3]octreotate analogue carrying a monocationic $^{99m}TcO_2^+$-tetraamine complex directly coupled at the N-terminus and easily obtained in high specific activities [15–17]. The above modification of [Tyr^3]octreotate has led to a very

Table 2. Biodistribution of [^{99m} Tc]Demotate 2 in Lewis rats bearing CA20948 tumours; data are presented as %ID/g±SD and results are the means of groups of four animals

Organ	Time			
	1 h	4 h	4 h (blockade)	24 h
Blood	0.13±0.02	0.01±0.00	0.01±0.00	0.00±0.00
Spleen	0.14±0.04^{++}	0.11±0.01^{+++}	0.14±0.01	0.05±0.00
Pancreas	8.43±0.19^{+}	8.60±1.25^{+}	0.37±0.08***	1.15±0.20^{+}
Adrenals	2.28±0.23	2.12±0.12^{+}	0.21±0.11***	0.62±0.09^{+++}
Kidney	2.97±0.23^{++}	3.67±0.16^{+++}	3.35±0.28	1.805±0.07
Liver	0.13±0.01^{+++}	0.09±0.00^{+++}	0.08±0.00	0.04±0.00
Stomach	0.75±0.09^{+}	0.70±0.06^{+++}	0.12±0.01***	0.11±0.01^{+}
Small intestine	0.18±0.02	0.29±0.34	0.03±0.01	0.04±0.01
Colon	1.26±0.01^{+++}	0.85±0.10^{+++}	0.08±0.02***	0.18±0.01^{+++}
Muscle	0.02±0.00	0.01±0.00	0.00±0.00	0.00±0.00
Femur	0.21±0.00	0.15±0.02	0.03±0.00	0.04±0.01
Thymus	0.12±0.01	0.10±0.01	0.05±0.00	0.03±0.00
Pituitary	1.30±0.016^{+++}	2.28±1.11	0.08±0.02**	0.79±0.01^{++}
Sternum	0.08±0.02	0.03±0.01	0.02±0.00	0.01±0.00
CA20948 tumour	2.52±0.03	2.86±0.45	0.39±0.07***	0.61±0.20^{+++}

Non-specific uptake was determined by co-injection of 500 μg octreotide (blockade)
**Very significant ($p<0.05$) and ***extremely significant ($p<0.005$) difference between blocked and unblocked animals (Student's *t* test)
$^{+/++}$ Significant/very significant ($p<0.05$) and $^{+++}$ extremely significant ($p<0.005$) difference compared with the respective values of [^{111} In] DOTA-tate (Table 3) (Student's *t* test)

Table 3. Biodistribution of [^{111} In]DOTA-tate in Lewis rats bearing CA20948 tumours; data are presented as %ID/g±SD and results are the means of groups of four animals

Organ	Time			
	1 h	4 h	4 h (blockade)	24 h
Blood	0.13±0.01	0.00±0.00	0.00±0.00	0.00±0.00
Spleen	0.05±0.00	0.01±0.00	0.02±0.00	0.01±0.00
Pancreas	7.65±0.49	6.31±0.85	0.33±0.024***	2.37±0.71
Adrenals	2.04±0.01	1.52±0.41	0.21±0.06***	1.33±0.01
Kidney	2.45±0.06	2.18±0.17	2.83±0.09***	2.16±0.41
Liver	0.06±0.01	0.02±0.00	0.02±0.01	0.02±0.00
Stomach	0.58±0.04	0.37±0.09	0.03±0.00***	0.19±0.05
Small intestine	0.15±0.02	0.41±0.15	0.02±0.00**	0.04±0.01
Colon	1.02±0.07	0.52±0.01	0.06±0.01	0.35±0.02
Muscle	0.02±0.00	0.00±0.00	0.00±0.00	0.00±0.00
Femur	0.17±0.02	0.076±0.00	0.01±0.00	0.04±0.01
Thymus	0.07±0.00	0.05±0.01	0.01±0.00	0.03±0.01
Pituitary	1.52±0.01	1.78±0.04	0.07±0.02***	0.95±0.08
Sternum	0.08±0.01	0.01±0.00	0.01±0.00	0.01±0.00
CA20948 tumour	2.44±0.23	3.06±0.94	0.37±0.02***	1.62±0.14

Non-specific uptake was determined by co-injection of 500 μg octreotide (blockade)
**Very significant (p<0.05) and ***extremely significant (p<0.005) difference between blocked and unblocked animals (Student's t test)

high affinity for the sst_2 in vitro and to a high target localisation in experimental animals [14]. Furthermore, when compared with the established radiopharmaceutical OctreoScan in a small number of sst_2-positive tumour patients, [^{99m}Tc]Demotate 1 demonstrated a much faster tumour localisation, thereby opening the possibility to implement a convenient 1-day clinical protocol [15, 16].

We were further interested to investigate to what extent the above promising qualities of [^{99m}Tc]Demotate 1 were related to the presence of the positive charge of the ^{99m}Tc-chelate in the immediate vicinity of [Tyr^3]octreotate. For this purpose, we synthesised [^{99m}Tc]Demotate 2, wherein an Asp residue—carrying a pendant negatively charged carboxylate group—has been introduced between the peptide chain and the monocationic ^{99m}Tc-chelate. It should be noted that similar modifications in cyclic octapeptide somatostatin analogues, such as the introduction of negatively charged residues close to/at their N-terminus, have been previously reported to favour renal clearance [30, 31]. In this study, the biological properties of [^{99m}Tc]Demotate 2 were compared with those of [^{111}In]DOTA-tate. The latter, besides also being a [Tyr^3]octreotate derivative, has so far shown a superior biological profile for receptor-targeted tumour imaging in comparison to the commercial radiotracer OctreoScan [14, 22, 23].

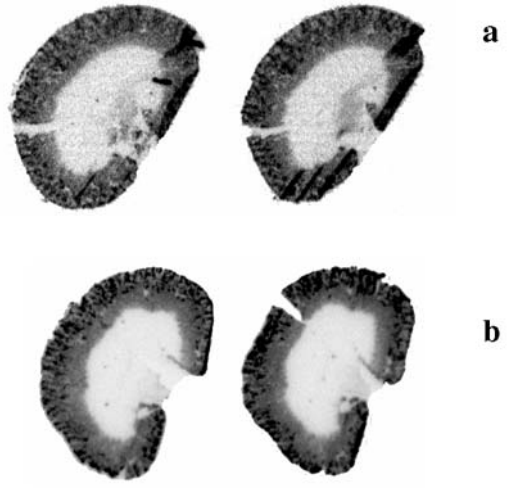

Fig. 5. Ex vivo autoradiographs of rat kidneys 4 h after injection of [^{99m}Tc]Demotate 2 (**a**) and 24 h after injection of [^{111}In]DOTA-tate (**b**)

As expected for a [Tyr^3]octreotate derivative, unlabelled Demotate 2 was shown to selectively bind with a high affinity to the human sst_2 stably expressed in cell preparations during receptor autoradiography assays. On the other hand, the binding affinities of all three non-metallated peptide conjugates Demotate 1, Demotate 2 and DOTA-tate for the rat sst_2 in rat brain cortex sections were all found to be in the lower nanomolar range, implying that the introduction of the Asp^0 in Demotate 2 had a minimal effect on its binding capacity. During labelling at room temperature under alkaline conditions, [^{99m}Tc]Demotate 2 was obtained in >98% yields and specific activities suitable for receptor-targeting applications (typically ~37 GBq ^{99m}Tc/μmol peptide). In a series of sst_2-positive cell lines, [^{99m}Tc]Demotate 2 and [^{111}In]DOTA-tate internalised with equal efficiency via an sst_2-mediated process. Study of the efflux of [^{99m}Tc]Demotate 2 and [^{111}In]DOTA-tate from CA20948 cells revealed that ~60% activity remained within the cells after 3-h incubation at 37°C. The mechanism of intracellular residualisation has not been investigated for these two compounds. However, studies on the intracellular fate of [^{111}In-DTPA^0]octreotide report that the

radiotracer, after being rapidly transported from the cell surface into lysosomes, is converted to peptide fragments trapped in the cell [28, 29]. It is very likely that a similar mechanism controls the residualisation of [^{99m}Tc]Demotate 2 and [^{111}In]DOTA-tate in CA20948 cells.

In Lewis rats bearing CA20948 tumours, [^{99m}Tc]Demotate 2 and [^{111}In]DOTA-tate showed high and receptor-mediated uptake in the tumour as well as in the sst_2-positive tissues (pancreas, pituitary and adrenals). The bulk of radioactivity was rapidly excreted from the body of rats into the urine via the kidneys and the urinary system. [^{111}In]DOTA-tate cleared more rapidly from background tissues, presumably as a result of its higher hydrophilicity. Although an extensive comparison of the hydrophilicity of the two radiotracers was not conducted in the present study, their respective HPLC profiles under identical chromatographic conditions revealed the higher hydrophilic character of [^{111}In]DOTA-tate (t_R=18.1 min versus 19.1 min for the ^{99m}Tc-peptide, Fig. 1). While the general biodistribution pattern again seems very similar for the two tracers, a few significant differences can be pointed out. Firstly, during the initial time intervals (1 and 4 h p.i.) [^{99m}Tc]Demotate 2 showed equally high or significantly higher uptake than [^{111}In]DOTA-tate in the tumour and the sst_2-positive tissues, like the pancreas, the adrenals, the pituitary and the gastrointestinal tract. In contrast, at 24 h p.i. most of [^{99m}Tc]Demotate 2 radioactivity has washed out significantly much faster from these tissues as compared with the ^{111}In tracer. Secondly, [^{111}In]DOTA-tate cleared more efficiently from background tissues than [^{99m}Tc]Demotate 2, resulting in high target-to-background ratios, as characteristically shown for the 4-h time interval in Fig. 6. In the kidneys, however, while in the initial time intervals [^{99m}Tc]Demotate 2 displayed significantly higher uptake than [^{111}In]DOTA-tate, at 24 h p.i. the values of the two peptides were practically the same, implying a faster renal washout of the ^{99m}Tc tracer for the period 4–24 h. It is interesting to note that the radioactivity distribution pattern of [^{99m}Tc]Demotate 2 and [^{111}In]DOTA-tate within the rat kidney was very similar. Thus, a similarly high accumulation of radioactivity predominantly localising in the renal cortex was observed. This finding implies a common course of radioactivity through kidney of the rat, which includes glomerular filtration and reabsorption in proximal tubule cells, as previously described for other radiolabelled somatostatin analogues [21]. It is very characteristic that this pattern has hardly changed at 24 h p.i. for the ^{111}In-peptide.

The faster renal washout observed in the case of [^{99m}Tc]Demotate 2 at the longer time intervals is reminiscent of its behaviour in the experimental tumour and in the physiological sst_2-positive sites and contrasts with the prolonged residence of [^{111}In]DOTA-tate in these tissues. The efflux profiles of the two tracers from CA20948 cells in vitro were found to be very similar at up to 3 h in this study, but efflux behaviour at longer time intervals (>4 h) was not investigated. It can be postulated that the radiotracers, after entering the cells either via a sst_2-specific process (tumour cells) or via another mechanism (rat kidney cells),

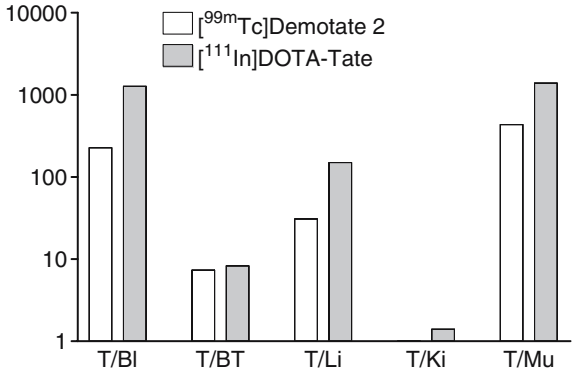

Fig. 6. Comparative tumour to non-target tissue ratios of [^{99m}Tc]Demotate 2 and [^{111}In]DOTA-tate at 4 h p.i. in CA20948 tumour-bearing Lewis rats. *T/Bl* tumour to blood, *T/BT* tumour to blocked tumour, *T/Li* tumour to liver, *T/Ki* tumour to kidneys, *T/Mu* tumour to muscle

are gradually metabolised in the lysosomes to different metabolic species. It is very probable that metabolites originating from [^{99m}Tc]Demotate 2 at periods >4 h cannot be retained in the cell as effectively as metabolites coming from [^{111}In]DOTA-tate. The validity of this hypothesis needs to be tested by further studies, especially if targeted therapy with ^{188}Re is considered [20]. While a shorter residence of radioactivity in the kidney is highly desirable, therapy can only benefit from it if retention in the tumour is not compromised.

Conclusion

It is clear from the above study, that [^{99m}Tc]Demotate 2 and [^{111}In]DOTA-tate show in general very similar behaviour in sst_2-positive cells and in CA20948 tumour-bearing rats. The ^{111}In-based radiopeptide shows faster clearance and longer residence in the tumour at longer time intervals. This advantage is somewhat compensated by its prolonged retention in the kidney.

However, considering the half-life of ^{99m}Tc, the availability of a rapidly localising ^{99m}Tc-based peptide radiotracer is highly desirable, as it would offer the prospect of implementing a logistically convenient 1-day clinical protocol. In view of this, [^{99m}Tc]Demotate 2 seems a very promising candidate for the scintigraphic detection of sst_2-positive lesions in man. Its potential usefulness as a diagnostic agent is currently being compared directly and in detail with that of [^{99m}Tc]Demotate 1. It is expected that the diagnostic value of either compound will be increased by the development of the respective ^{188}Re-based therapeutic drug ([^{188}Re]Demotate 1 or 2), and work towards this direction is in progress.

Acknowledgements. Financial support of Dr. T. Maina's Short-Term Scientific Mission to Rotterdam by the E.U. through COST Action B12: "Radiotracers for In Vivo Assessment of Biological Function", WG-3: "Radiolabelled Biologically Active Peptides" is gratefully acknowledged.

References

1. Kwekkeboom DJ, Krenning EP. Somatostatin receptor imaging. Semin Nucl Med 2002;32:84–91
2. Breeman WAP, de Jong M, Kwekkeboom DJ, Valkema R, Bakker WH, Kooij PPM, et al. Somatostatin receptor-mediated imaging and therapy: basic science, current knowledge, limitations and future perspectives. Eur J Nucl Med Mol Imaging 2001;28:1421–1429
3. de Jong M, Kwekkeboom D, Valkema R, Krenning EP. Radiolabeled peptides for tumour therapy: current status and future directions. Plenary lecture at the EANM 2002. Eur J Nucl Med Mol Imaging 2003;30:463–469
4. Reubi JC, Schär JC, Waser B, Wenger S, Heppeler A, Schmitt JS, et al. Affinity profiles for human somatostatin receptor subtypes sst_1–sst_5 of somatostatin radiotracers selected for scintigraphic and radiotherapeutic use. Eur J Nucl Med Mol Imaging 2000;27:273–282
5. de Jong M, Breeman WAP, Valkema R, Bernard BF, Krenning EP. Combination radionuclide therapy using ^{177}Lu- and ^{90}Y-labeled somatostatin analogs. J Nucl Med 2005;46:13S–17S
6. Kwekkeboom DJ, Müller-Brand J, Paganelli G, Anthony LB, Pauwels S, Kvols LK, et al. Overview of results of peptide receptor radionuclide therapy with 3 radiolabeled somatostatin analogs. J Nucl Med 2005;46:62S–66S
7. Krenning EP, Valkema R, Kwekkeboom DJ, de Herder WW, van Eijck CHJ, de Jong M, et al. Molecular imaging as in vivo molecular pathology for gastroenteropancreatic neuroendocrine tumors: implications for follow-up after therapy. J Nucl Med 2005;46:76S–82S
8. Liu S, Edwards DS. ^{99m}Tc-labeled small peptides as diagnostic radiopharmaceuticals. Chem Rev 1998;58:437–441
9. Schibli R, Schubiger PA. Current use and future potential of organometallic radiopharmaceuticals. Eur J Nucl Med Mol Imaging 2002;29:1529–1542
10. Shih WJ, Hirschowitz E, Bensadoun E, Woodring J, Ryo YU, Kraman S. Biodistribution on Tc-99 m labeled somatostatin receptor-binding peptide (Depreotide, NeoTec) planar and SPECT studies. Ann Nucl Med 2002;16:213–219
11. Shih WJ, Kiefer V. Radiation therapy of changes secondary to lung cancer and pneumonectomy on bone and Tc-99 m depreotide imaging. Clin Nucl Med 2003;28:419–420
12. Gabriel M, Decristoforo C, Donnemiller E, Ulmer H, Watfah Rychlinski C, Mather SJ, et al. An intrapatient comparison of ^{99m}Tc-EDDA/HYNIC-TOC with ^{111}In-DTPA-octreotide for diagnosis of somatostatin receptor-expressing tumors. J Nucl Med 2003;44:708–716
13. Plachcinska A, Mikolajczak R, Maecke HR, Mlodkowska E, Kunert-Radek J, Michalski A, et al. Clinical usefulness of ^{99m}Tc-EDDA/HYNIC-TOC scintigraphy in oncological diagnostics: a preliminary communication. Eur J Nucl Med Mol Imaging 2003;30:1402–1406
14. Storch D, Béhé M, Walter M, Chen J, Powell P, Mikolajczak R, et al. Evaluation of [^{99m}Tc/EDDA/HYNIC^0]octreotide derivatives compared with [^{111}In-DOTA^0,Tyr^3,Thr^8]octreotide and [^{111}In-DTPA^0]octreotide: does tumor or pancreas uptake correlate with the rate of internalization? J Nucl Med 2005;46:1561–1569
15. Maina T, Nock B, Nikolopoulou A, Sotiriou P, Loudos G, Maintas D, et al. [^{99m}Tc]Demotate, a new ^{99m}Tc-based [Tyr^3] octreotate analogue for the detection of somatostatin receptor-positive tumours: synthesis and preclinical results. Eur J Nucl Med Mol Imaging 2002;29:742–753
16. Decristoforo C, Maina T, Nock B, Gabriel M, Cordopatis P, Moncayo R. ^{99m}Tc-Demotate 1: first data in tumour patients-results of a pilot/phase I study. Eur J Nucl Med Mol Imaging 2003;30:1211–1219
17. Gabriel M, Decristoforo C, Maina T, Nock B, vonGuggenberg E, Cordopatis P, et al. ^{99m}Tc-N_4-[Tyr^3]octreotate versus ^{99m}Tc-EDDA/HYNIC-[Tyr^3]octreotide: an intrapatient comparison of two novel technetium-99 m labeled tracers for somatostatin receptor scintigraphy. Cancer Biother Radioph 2004;19:73–79
18. Mantegazzi D, Ianoz E, Lerch P, Nicolò F, Chapuis G. Preparation and crystal structure of polymeric lithium[dioxoTc(V)-tetraazaundecane]-bis(trifluoromethanesulfonate) complex. Inorg Chim Acta 1990;176:99–105
19. Parker D, Roy PS. Synthesis and characterization of stable Re(V) dioxo complexes with acyclic tetraamine ligands, $[LReO_2]^+$. Inorg Chem 1988;27:4127–4130
20. Bläuenstein P, Pfeiffer G, Schubiger PA, Anderegg G, Zollinger K, May K, Proso Z, Ianovici E, Lerch P. Chemical and biological properties of a cationic Tc-tetraamine complex. Int J Appl Radiat Isot 1985;36:315–317
21. Prakash S, Went MJ, Blower PJ. Cyclic and acyclic polyamines as chelators of rhenium-186 and rhenium-188 for therapeutic use. Nucl Med Biol 1996;23:543–549
22. de Jong M, Breeman WAP, Bernard BF, Bakker WH, Schaar M, van Gameren A, et al. [^{177}Lu-DOTA^0,Tyr^3]octreotate for somatostatin receptor-targeted radionuclide therapy. Int J Cancer 2001;92:628–633
23. Kwekkeboom DJ, Bakker WH, Kooij PP, Konijnenberg MW, Srinivasan A, Erion JL, et al. [^{177}Lu-DOTA^0,Tyr^3]octreotate: comparison with [^{111}In-DTPA^0]octreotide in patients. Eur J Nucl Med Mol Imaging 2001;28:1319–1325
24. Breeman WAP, de Jong M, Visser TJ, Erion JL, Krenning EP. Optimising conditions for radiolabeling of DOTA-peptides with ^{90}Y, ^{111}In and ^{177}Lu at high specific activities. Eur J Nucl Med Mol Imaging 2003;30:917–920
25. Hofland LJ, Breeman WA, Krenning EP, de Jong M, Waaijers M, van Koetsveld PM, et al. Internalization of [DOTA^0,^{125}I-Tyr^3]octreotide by somatostatin receptor-positive cells in vitro and in vivo: implications for somatostatin receptor-targeted radio-guided surgery. Proc Assoc Am Phys 1999;111:63–69
26. Bernard BF, Krenning E, Breeman WAP, Visser TJ, Bakker WH, Srinivasan A, et al. Use of the rat pancreatic CA20948 cell line for the comparison of radiolabeled peptides for receptor-targeted scintigraphy and radionuclide therapy. Nucl Med Commun 2000;21:1079–1085
27. Taylor JE, Theveniau MA, Bashirzadeh R, Reisine T, Eden PA. Detection of somatostatin receptor subtype 2 (SSTR2) in established tumors and tumor cell lines: evidence for SSTR2 heterogeneity. Peptides 1994;15:1229–1236
28. Froidevaux S, Hintermann E, Török M, Mäcke HR, Beglinger C, Eberle AN. Differential regulation of somatostatin receptor type 2 (sst 2) expression in AR4-2J tumor cells implanted into mice during octreotide treatment. Cancer Res 1999;59: 3652–3657
29. Duncan JR, Stephenson MT, Wu HP, Anderson CJ. Indium-111-diethylenetriaminepentaacetic acid-octreotide is delivered in vivo to pancreatic, tumor cell, renal, and hepatocyte lysosomes. Cancer Res 1997;57:659–671
30. Akizawa H, Arano Y, Uezono T, Ono M, Fujioka Y, Uehara T, Yokoyama A, Akaji K, Kiso Y, Koizumi M, Saji H. Renal metabolism of ^{111}In-DTPA-D-Phe^1-octreotide in vivo. Bioconjugate Chem 1998;9:662–670
31. Akizawa H, Arano Y, Mifune M, Iwado A, Saito Y, Mukai T, et al. Effect of molecular charges on renal uptake of ^{111}In-DTPA-conjugated peptides. Nucl Med Biol 2001;28:761–768